

Mainshock-Aftershock Ground Motion Features and Their Influence in Building's Seismic Response

JORGE RUIZ-GARCÍA

Facultad de Ingeniería Civil, Universidad Michoacana de San Nicolás de Hidalgo, Morelia, México

This article presents the results of examining ground motion characteristics in 184 real mainshock-aftershock earthquake ground motions. It is shown that the predominant period (a measure of the frequency content) of the set of mainshocks tends to be longer than that of the corresponding aftershocks. It is highlighted that the response of structures under artificial sequences is very different from that of real sequences, particularly when the approach of repeating the real mainshock with identical ground motion features as an artificial aftershock is employed. It is also demonstrated that the predominant period of the aftershock significantly influences the post-mainshock response.

Keywords Aftershocks; Frequency Content; Seismic Sequences; Artificial Sequences; Permanent Displacement

1. Introduction

Man-made structures located in earthquake-prone regions are not exposed to a single seismic event, but also to a seismic sequence consisting of foreshocks, the mainshock, and aftershocks. Aftershock events are triggered by the mainshock due to both static stress and dynamic (transient) stress changes occurring during the earthquake process (e.g., [Aki, 1984](#); [Harris, 1998](#); [Dalguer et al., 2004](#)). In particular, seismologists have noted that the rupture of asperities and barriers in a fault (i.e., according to [Aki, 1984](#), they are strong patches of the fault plane that are resistive to breaking, which explains the irregular slip motion over a heterogenous fault plane) triggers aftershocks. That is, an asperity/barrier release the stress concentration caused by the mainshock in the surrounding area and, as a consequence, it triggers the aftershock. In fact, larger asperity areas are related to large earthquakes (e.g., [Ruff and Kanamori, 1983](#)).

Based on statistics of mainshock-aftershocks scenarios from different seismogenic regions, three empirical scaling laws have been proposed for characterizing the occurrence of aftershocks (e.g., [Shcherbakov 2005](#)): (1) Gutenberg-Richter, for the frequency-magnitude relationship of the aftershocks; (2) the Modified Omori's law, for the time decay in the rate of aftershock occurrence; and (3) Bath's law, for the relationship between the mainshock earthquake magnitude and its corresponding main aftershock earthquake magnitude. Parameters for defining each scaling law can be found depending on the statistical properties of particular seismic sequences as shown in [Shcherbakov et al. \[2005\]](#). In particular, the empirical Bath's law states that the average difference in magnitude between a mainshock and its largest aftershock is constant (typically 1.2), regardless of the mainshock

Received 26 August 2011; accepted 27 January 2012.

Address correspondence to Jorge Ruiz-García, Facultad de Ingeniería Civil, Universidad Michoacana de San Nicolás de Hidalgo, Edificio C, Planta Baja, Cd. Universitaria, Morelia 58040, México. E-mail: jruizgar@stanfordalumni.org

magnitude, which imply that mainshocks have larger asperity areas and seismic moment, M_o , than their aftershocks.

From an engineering point of view, earthquake ground motions recorded in accelerographic stations are of paramount importance for developing dynamic time-history analyses of structures. The most important characteristics to describe an earthquake ground motion are the amplitude, the frequency content, and the duration of the motion (e.g., Kramer, 1991). Both the mainshock and the corresponding aftershock earthquake ground motions can be described from ground motion parameters that reflect the aforementioned characteristics. For example, examining one single mainshock and its largest aftershock, Dunbar and Charlwood [1991] stated that “large magnitude events generate ground motion rich in low frequencies while small magnitude events generate ground motion rich in high frequencies.” To support their statement, the authors illustrated the acceleration time-history of the mainshock and the corresponding aftershock recorded in station C-00 in Taiwan on July 30, 1986. The authors also pointed out that “the difference in the frequency content of these two accelerograms is *evident*.” This statement could be explained since a mainshock fractures a larger asperity area (i.e., the area on the fault plane that triggers the rupture in the fault) than the asperity areas that causes the following aftershocks. The studies by Dalguer and Irikura [2002] as well as Miyake *et al.* [2002] suggest that low-frequency ground motions are related to a bigger size of asperity area and smaller stress drop than that of high-frequency ground motions. This means that large earthquakes generate ground motion waves that are richer in low frequencies.

The response of structures subjected to mainshock-aftershock earthquake ground motion sequences has gained the attention from the earthquake engineering community recently, since strong aftershocks might be triggered after the mainshock. For example, after the 1994 Northridge earthquake ($M_w = 6.7$) that affected the Los Angeles Area in California, an $M_w = 6.0$ aftershock was felt approximately 1 min later [Dreger, 1996]. Likewise, after the mainshock ($M_w = 8.8$) on February 27, 2010 that struck the central-southern region of Chile, 306 aftershocks having magnitudes greater than 5.0 were recorded between February 27 and April 26. Among them, 21 aftershocks had magnitude greater than 6.0 [USGS, 2010]. Hereafter, the aftershock ground motion is denoted for the acceleration time-history recorded during the largest aftershock. As a historical note, in the author’s knowledge, the first pioneering analytical study of nonlinear single-degree-of-freedom (SDOF) systems subjected to mainshock-aftershock acceleration time histories recorded during the 1972 Managua earthquake were performed by Mahin [1980]. He observed that the displacement ductility demand, μ (i.e., peak inelastic displacement normalized with respect to the system’s yield displacement) of elastoplastic SDOF systems slightly increased at the end of the main aftershock with respect to the mainshock. Years later, while some of the following studies have been focused on the nonlinear response of SDOF systems (e.g., Amadio *et al.*, 2003; Luco *et al.*, 2004; Hatzigeorgiou and Beskos, 2009; Hatzigeorgiou, 2010), others have focused their attention in the response of multiple-degree-of-freedom (MDOF) systems (e.g., Fragiocomo *et al.*, 2004; Lee and Foutch; 2004; Li and Ellingwood, 2007; Ruiz-García *et al.*, 2008; Hatzigeorgiou and Liolios, 2010; Ruiz-García and Negrete-Manriquez, 2011; Erochko *et al.*, 2011). Most of the previous studies employed artificial seismic sequences instead of real (i.e., as-recorded) mainshock-aftershocks sequences to evaluate the structural seismic response. They employed artificial sequences using the mainshock acceleration time-history as a seed for simulating the following aftershocks using the approaches: (1) back-to back, or repeated, approach (e.g., Amadio *et al.*, 2003; Fragiocomo *et al.*, 2004; Lee and Foutch; 2004; Li and Ellingwood, 2007; Hatzigeorgiou and Beskos, 2009; Erochko *et al.*, 2011); or (2) randomized approach (e.g., Luco *et al.*, 2004; Li and Ellingwood, 2007; Hatzigeorgiou, 2010; Hatzigeorgiou

and Liolios, 2010). The first approach consists on repeating the real mainshock, at scaled or identical amplitude, as an artificial aftershock, which assumes that the ground motion features such as frequency content and strong motion duration of the mainshock and aftershock(s) are the same. Lee and Foutch [2004] and Li and Ellingwood [2007] made an effort of taking into account the aftershock hazard level by scaling down the amplitude of the second ground motion. However, as explained above, this seismic scenario is unrealistic since the mainshock and the largest aftershock are related to different asperity areas and, as a consequence, they have different frequency content. The second approach consists on ensemble a set of real mainshocks, and generating artificial sequences by selecting a mainshock and simulating the remaining aftershocks by repeating the mainshock waveform repeatedly, at reduced or identical amplitude, with no change in spectral content as an artificial aftershock. For example, following the methodology proposed by Sunasaka and Kiremidjian [1983], Li and Ellingwood [2007] determined a scale factor of 0.9 for representing an aftershock hazard level of 15% probability of exceedance in 50 years in a set of 20 earthquake ground motions having exceedance probability of 10% in 50 years.

It should be noted that although previous studies developed extensive analytical studies and provided information of the response of structures to seismic sequences, the use of artificial seismic sequences, either generated from the repeated or the randomized approach, could lead to misunderstand the structural response under real seismic sequences. This situation might occur if the relationships of the ground motion characteristics between the mainshock and the following aftershocks are not properly represented in the artificial sequences. Therefore, the main objectives of the investigation reported in this paper were three-fold: (1) to characterize the ground motion features (i.e., amplitude, frequency content, and strong-motion duration) of 184 mainshock-largest aftershock ground motion sequences recorded during 13 earthquakes around the world; (2) to identify the relationships between the ground motion features of recorded mainshock-aftershocks; and (3) to investigate the impact of the frequency content relationship between the mainshock-aftershock in the dynamic response of frame buildings.

2. Mainshock-Aftershock Ground Motion Database

Available strong motion databases, such as the Mexican Database of Strong Motions [MDSG, 1999] and the Pacific Earthquake Engineering NGA Database [PEER, 2011] provide a good opportunity for identifying acceleration time-histories of recorded mainshocks and their corresponding largest aftershocks. The following criteria were established for selecting the set of mainshock-aftershock earthquake ground motions employed in this study.

2.1. Mainshock-Aftershock Sequences from MDSG Database

Existing structures located in the Mexican Pacific coast are threatened by subduction interface earthquakes. This zone corresponds to seismic zone D (i.e., having the highest seismic hazard in Mexico) according to the Manual for Design of Civil Works [MDCW, 1993]. Therefore, an ensemble of ground motion seismic sequences was assembled from the Mexican Database of Strong Motions (MDSG) [1999]. Seismic sequences including the mainshock and at least one aftershock recorded from 1960–1999 were identified from the database. First, around 500 seismic sequences were gathered. Next, seismic sequences were selected according to the following criteria: (1) magnitude of mainshock event equal to or greater than 5.5, whereas magnitude of the aftershock event equal to or greater than 4.0;

(2) available information about the soil condition, which correspond to Soil Type I (i.e., bedrock and stiff soils such as compacted volcanic ashes, moderately cemented sandstones, and highly compacted clays; MDCW, 1993); (3) acceleration time histories recorded on stations placed on free field or low-height buildings for which soil-structure interaction effects were negligible; and (4) seismic sequences having peak ground acceleration (PGA) of one of the mainshock horizontal components greater than 100 cm/s^2 . Under these criteria, 26 seismic sequences from 2 orthogonal horizontal components recorded during 5 historical earthquakes, including 7 sequences from the 1985 Michoacan earthquake ($M_w = 8.0$), were selected for this investigation. Some sequences have more than one aftershock ground motion.

For illustration purposes, Fig. 1 shows four seismic sequences included in the database. For performing dynamic analysis, there is a time-gap having zero acceleration ordinates between the mainshock and the aftershock acceleration time-history to ensure that the systems reach its rest position, whereas duration of the aftershock acceleration time-history included zero acceleration ordinates at the end of the excitation. Similarly, the power amplitude spectrum computed for the example sequences is shown in Fig. 2.

It should be noted that in three stations, the intensity of the largest aftershock, measured by the PGA, was greater than that of the corresponding mainshock, although the magnitude and seismic moment of the mainshock was greater than that of the aftershock [Astiz *et al.*, 1987]. As examples, seismic sequences PAPAN850919 and AZIH850919 recorded in stations located at Papanoa town and Zihuatanejo Airport during the mainshock (September 19, 1985, $M_s = 8.1$) and the main aftershock (September 21, 1985, $M_s = 7.6$) are shown in Fig. 1. This could be explained since the epicenter of the largest aftershock was closer to the recording stations than that of the mainshock (i.e., rupture triggered by the September 19 event propagated to the southeast portion of the Michoacan gap).

2.2. Mainshock-Aftershock Sequences from PEER NGA Database

The following criteria were employed for identifying and selecting mainshock-aftershock seismic sequences from the Pacific Earthquake Engineering NGA database [PEER, 2010]: (1) magnitude of main aftershock event equal to or greater than 4.0; (2) available information about the soil condition, which correspond to Soil Type A, B, C, or D (i.e., bedrock and stiff soils); (3) acceleration time histories recorded on stations placed on free field or low-height buildings where soil-structure interaction effects are negligible; and (4) seismic

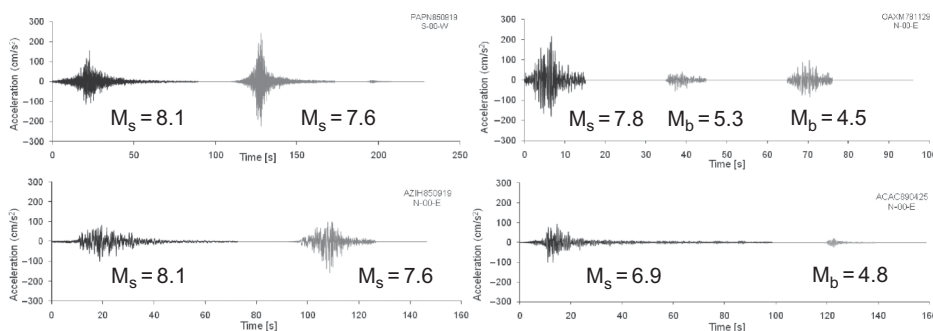


FIGURE 1 Examples of seismic sequences recorded in the Mexican Pacific coast from subduction interface earthquakes.

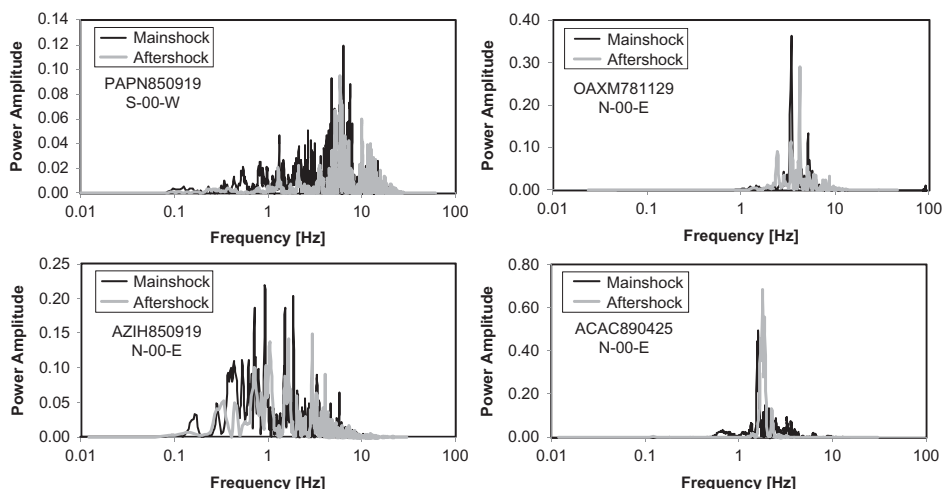


FIGURE 2 Examples of power amplitude spectrum of mainshock-aftershock sequences recorded in the Mexican Pacific coast from subduction interface earthquakes.

sequences having PGA of the mainshock horizontal component greater than 100 cm/s^2 and PGA of the aftershocks greater than 50 cm/s^2 .

Under the aforementioned criteria, a total of 158 mainshock-aftershocks sequences, from 2 orthogonal horizontal components, were identified in this study. Among them, 100 seismic sequences were gathered from accelerographic stations placed in California, which corresponds to 58 seismic sequences from the 1994 Northridge earthquakes, 30 from the 1979 Imperial Valley earthquakes, 6 from the 1980 Mammoth Lakes earthquakes, and 2 from the 1961 Hollister, the 1980 Livermore, and the 1983 Coalinga earthquakes. In addition, 10 seismic sequences were obtained from the 1980 Irpinia (Italy) earthquakes and 48 from the CHY accelerographic array during the 1999 Chi-Chi (Taiwan) earthquakes. Table 1 reports relevant information about the selected seismic sequences. It should be mentioned that some sequences have more than one aftershock ground motion that met the aforementioned criteria.

An interesting distinct feature from previous studies is that the catalogue contains 14 seismic sequences captured in accelerographic stations located near the causative fault during the 1994 Northridge earthquakes. For example, seismic sequences recorded at well-known Rinaldi Receiving Station and Sylmar Converter Station located in the Los Angeles Area were considered in this study. Examples of accelerograms from near-fault seismic sequences are illustrated in Fig. 3, while corresponding power spectrum is shown in Fig. 4.

3. Relationship between Mainshock-Aftershock Ground Motion Parameters

In order to study whether the selected aftershock acceleration time-histories have similar ground motion characteristics to their corresponding mainshock time-histories, the following parameters were identified from each accelerogram: (1) the predominant period of the ground motion (T_g); (2) the bandwidth (Ω); and (3) the effective duration (t_D). The predominant period of the ground motion was defined as the period at which the maximum ordinate of a five percent damped relative velocity spectrum occurs [Miranda, 1993]. In addition, using the concept developed by Vanmarcke [1972], an analog measure of the

TABLE 1 Seismic sequences selected from the Pacific Earthquake Engineering (PEER) database

Earthquake name	Date	Time	M ^a	No. of sequences
Hollister	4/9/61	07:23	5.6	2
	4/9/61	07:25	5.5	
Imperial Valley	15/10/79	23:16	6.5	30
	15/10/79	23:19	5.0	
Livermore	1/27/80	19:00	5.8	2
	1/29/80	02:33	5.4	
Mammoth Lakes	05/25/80	16:34	6.1	6
	05/25/80	16:49	5.7	
	05/25/80	19:44	5.9	
	05/25/80	20:35	5.7	
	05/26/80	18:58	5.7	
	05/27/80	14:51	5.9	
Irpinia, Italy	11/23/80	19:34	6.9	10
	11/23/80	19:35	6.2	
Coalinga	07/22/83	23:42	6.4	2
	07/25/83	2:39	5.8	
Northridge	01/17/94	12:31	6.7	58
	01/17/94	12:32	6.0	
	03/20/94	21:20	5.3	
Chi-Chi, Taiwan	9/20/99	09:20	7.6	48
	9/20/99	17:57	5.9	
	9/20/99	18:03	6.2	
	9/22/99	00:14	6.2	
	9/25/99	23:52	6.3	

^aMagnitude reported in the PEER NGA strong motion database.

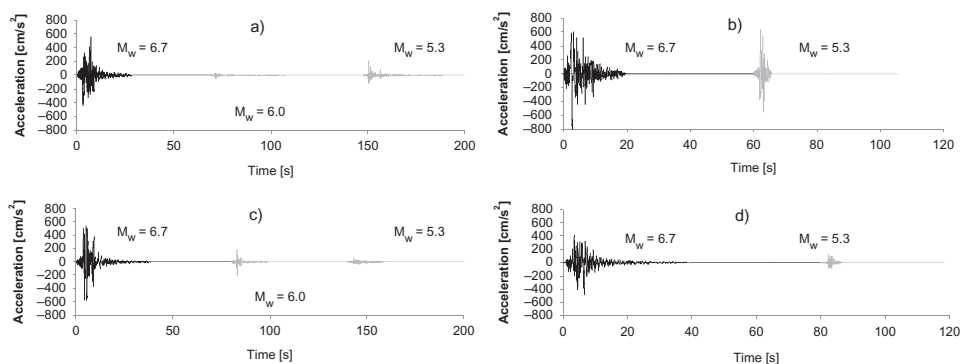


FIGURE 3 Examples of near-fault seismic sequences considered in this study: (a) Jensen Filter Plant station (comp. 22); (b) Rinaldi Receiving station (comp. 228); (c) Newhall station (comp. 180); and (d) Sylmar Converter Station (comp. 288).

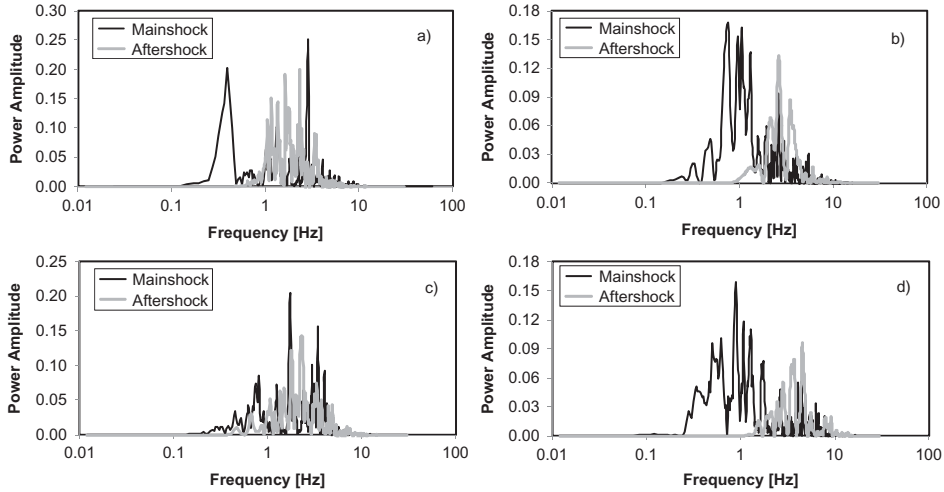


FIGURE 4 Examples of power amplitude spectrum from near-fault seismic sequences considered in this study: (a) Jensen Filter Plant station (comp. 22); (b) Rinaldi Receiving station (comp. 228); (c) Newhall station (comp. 180); and (d) Sylmar Converter Station (comp. 288).

ground motion spread about the central period, or bandwidth, as a function of the spectral parameters computed for the squared velocity spectra was defined as follows:

$$\Omega = \left[1 - \frac{(\lambda_1^*)^2}{\lambda_0^* \lambda_1^*} \right]^{\frac{1}{2}}, \quad (1)$$

where the spectral parameters λ_0^* , λ_1^* , and λ_2^* were computed from the squared velocity spectra for elastic SDOF systems having damping ratio of 5% as follows:

$$\lambda_0^* = \sum_{i=1}^n S_{v,i}^2 \cdot \Delta T \quad (2)$$

$$\lambda_1^* = \sum_{i=1}^n T_i \cdot S_{v,i}^2 \cdot \Delta T \quad (3)$$

$$\lambda_2^* = \sum_{i=1}^n T_i^2 \cdot S_{v,i}^2 \cdot \Delta T. \quad (4)$$

According to the definition postulated by Vanmarcke [1972], small values of the bandwidth are associated with narrow band signals and, thus, bandwidth allows defining whether a ground motion has narrowband or broadband frequency content around its central frequency or central period. In addition, the measure of strong ground motion duration defined by Trifunac and Brady [1975] was employed in this study. Trifunac and Brady [1975] defined significant strong motion duration, t_D , as the time interval from 5–95% of the Arias intensity computed from each single acceleration time-history. Therefore, values of T_g , Ω , and t_D corresponding to each mainshock-aftershock sequence were computed as part of this study. For illustration purposes, estimation of T_g from the velocity spectra of three pairs of mainshock-largest aftershock ground motions from the 1995 Northridge earthquake is shown in Fig. 5.

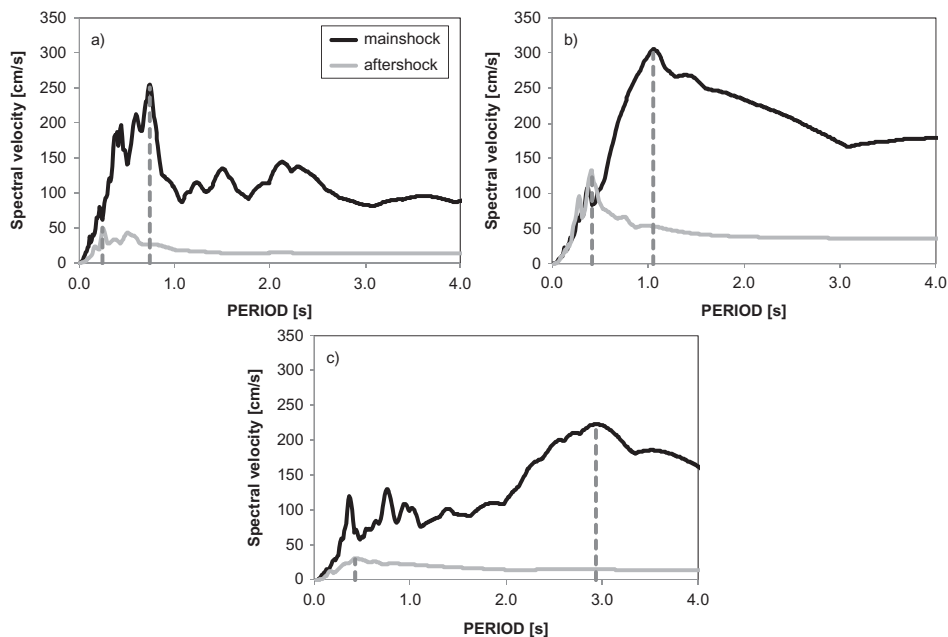


FIGURE 5 Estimation of predominant period of the ground motion from the velocity spectra of typical mainshock-largest aftershock recorded during the 1994 Northridge earthquake: (a) Tarzana (comp. 090); (b) Rinaldi (comp. 228); and (c) Jensen Filter Plant Generator (comp. 022).

3.1. Frequency Content Relationships

After examining the mainshock-aftershock ground motions gathered from the subduction zone of the Mexican Pacific coast, it was noted that the predominant periods of mainshocks were longer than those of the corresponding aftershocks in about 65% of the sequences, with increasing percentage for the 1985 earthquakes. This can be explained since the seismic moment of the September 19, 1985 mainshock was $7.2 \pm 1.6 \times 10^{27}$ dyne-cm, while the September 21, 1985 aftershock was 1.2×10^{27} dyne-cm [Astiz, *et al.*, 1987], which suggest that larger asperity area was fractured during the mainshock than in the aftershock. The relationship between T_g and Ω for all 26 mainshock-aftershock ground motions recorded in the subduction zone of the Mexican Pacific coast is shown in Fig. 6a. From this figure, it can be observed that the predominant period of the mainshocks follows a linear trend with respect to its bandwidth (e.g., T_g decreases as Ω increases). However, it should be noted that the relationship between T_g and Ω for the aftershocks does not follow a clear linear trend. The relationship between the predominant period of the ground motion corresponding to each mainshock, $T_{g,M}$, and its corresponding largest aftershock, $T_{g,MA}$, is also shown in Fig. 6b. The sample correlation coefficient computed for this relationship is 0.51, which leads to the conclusion that the predominant period of the mainshocks is only mildly linear correlated, from a statistical point of view, with the dominant period of their largest aftershocks.

The relationships between T_g and Ω for mainshock and largest aftershock ground motions recorded during the 1979 Imperial Valley, 1980 Mammoth Lakes, and 1994 Northridge earthquakes are shown in Figs. 7a–d. Distinction between far-field and near-fault ground motions (i.e., 44 far-field and 14 near-fault earthquake ground motions)

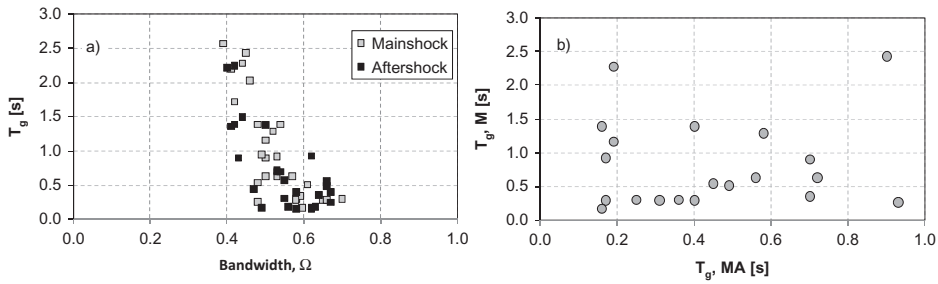


FIGURE 6 (a) Relationship between the predominant period of the ground motion, T_g , and bandwidth, Ω , obtained from the set of interface subduction mainshocks and corresponding main aftershocks, and (b) relationship between the predominant periods of the mainshocks ($T_{g,M}$) and their corresponding aftershocks ($T_{\downarrow}(g, MA)$).

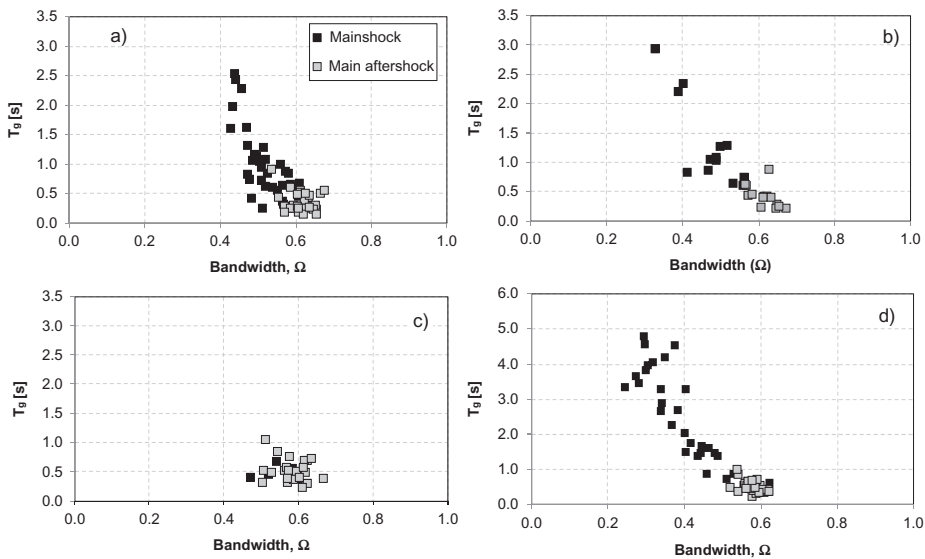


FIGURE 7 Relationship between T_g and Ω for mainshocks and their largest aftershocks: (a) 1994 Northridge earthquakes (far-field ground motions); (b) 1994 Northridge earthquakes (near-fault ground motions); and (c) 1980 Mammoth Lakes earthquakes, d) 1979 Imperial Valley earthquakes.

in the Northridge earthquake is noted in Figs. 7a and b. For these seismic scenarios, it was found that mainshock ground motions from the 1994 Northridge earthquake have predominant periods longer than those of their largest aftershock ground motions in 93% of the sequences, while for the 1979 Imperial Valley and the 1980 Mammoth Lakes earthquakes were 93% and 50% of the sequences. In addition, from the figures, it can be seen that for the three seismic scenarios, the relationship between T_g and Ω is different for the set of mainshock and corresponding aftershocks. For instance, for the 1979 Imperial Valley earthquakes: (1) the predominant period of the mainshocks follows a linear trend with respect to its bandwidth (e.g., T_g decreases as Ω increases); and (2) predominant periods as well as bandwidth of the largest aftershock ground motions tend to be shorter than the predominant period of mainshock ground motions. According with the definition postulated in [Vanmarcke, 1972], large values of the bandwidth (e.g., larger than about 0.5) are associated

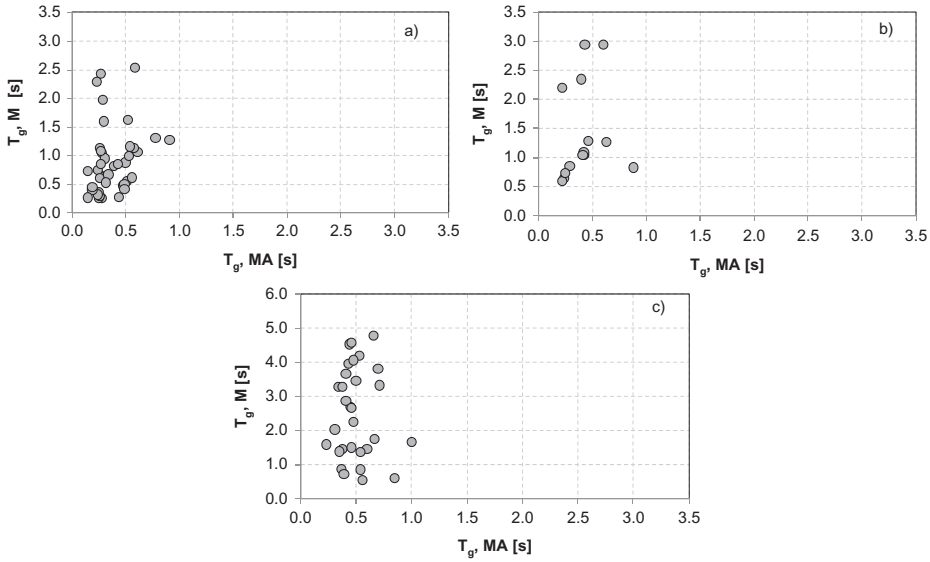


FIGURE 8 Relationship of $T_{g,M}$ and $T_{g,MA}$ for three Californian earthquakes: (a) 1994 Northridge earthquakes (far-field ground motions); (b) 1994 Northridge earthquakes (near-fault ground motions); and (c) 1979 Imperial Valley earthquakes.

with broad band signals. That is, aftershock ground motions recorded during the Northridge and the Imperial Valley earthquakes are richer in higher frequencies than mainshock ground motions, which is consistent with seismological studies (i.e. higher frequencies are generated from fracturing small asperities). For instance, the seismic moment of the January 17, 1994 Northridge earthquakes was 1.2×10^{26} dyne-cm [Thio and Kanamori, 1996; PEER, 2011], while the seismic moment of the March 20, 1994 Northridge aftershock was 1.2×10^{24} dyne-cm [Mori *et al.*, 2003].

In addition, the relationship between $T_{g,M}$ and $T_{g,MA}$ is also shown in Figs. 8a–d for the seismic sequences recorded during the Californian earthquakes. The sample correlation coefficient computed for these cases is 0.18, 0.15, and -0.05 , respectively, which also means that the predominant periods of the mainshock and aftershock ground motions are weakly correlated from a statistical point-of-view.

Next, Figs. 9 and 10 illustrates the relationships T_g vs. Ω and $T_{g,M}$ vs. $T_{g,MA}$ corresponding to the 1980 Irpinia (Italy) earthquakes and the 1999 Chi-Chi (Taiwan) earthquakes. For these earthquakes, it was found that the predominant period of the mainshock ground motion was longer than that of the aftershocks in 80% and 65% of the examined sequences for the Irpinia and Chi-Chi earthquakes, respectively. It should be noted that in the 1980 Irpinia earthquakes, the mainshock had a seismic moment of 2.51×10^{26} dyne-cm, while the largest aftershock had a seismic moment of 2.24×10^{25} dyne-cm [PEER, 2011]. Unlike the Californian seismic scenarios, the trend of T_g vs. Ω for mainshock and aftershock earthquake ground motions is approximately similar. However, the correlation between $T_{g,M}$ and $T_{g,MA}$ is also weakly correlated as in the Californian sequences.

3.2. Strong-Motion Duration Relationships

The relationship between the strong-motion duration, measured by the definition given in Trifunac and Brady [1975], of the mainshock and corresponding largest aftershocks for

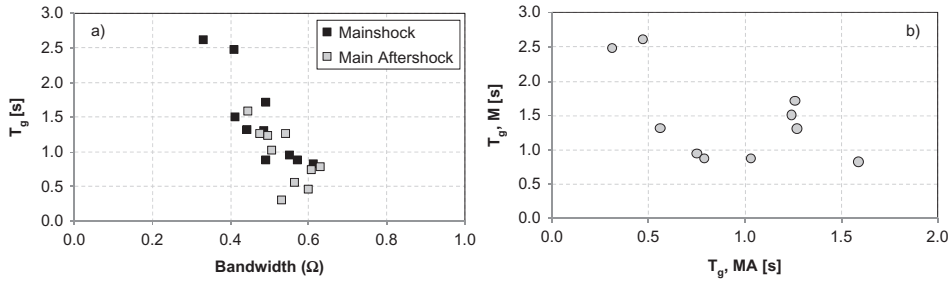


FIGURE 9 (a) Relationship between the predominant period of the ground motion, T_g , and bandwidth, Ω , obtained from the 1980 Irpinia, Italy, mainshocks and corresponding largest aftershocks; and (b) relationship between the predominant periods of the mainshocks ($T_{g,M}$) and their corresponding aftershocks ($T_{g,MA}$).

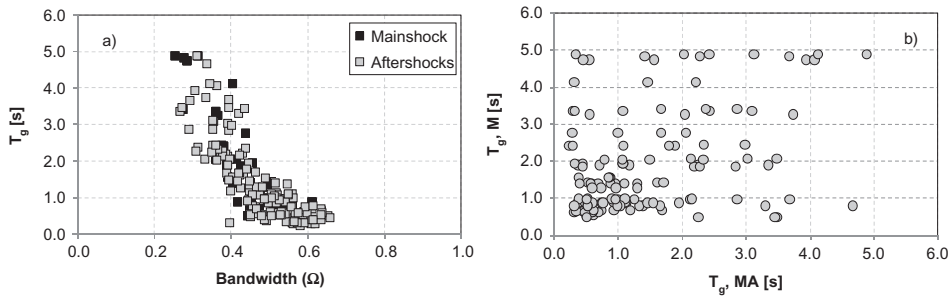


FIGURE 10 (a) Relationship between the predominant period of the ground motion, T_g , and bandwidth, Ω , obtained from the CHY accelerographic array during the 1999 Chi-Chi, Taiwan, mainshocks and corresponding main aftershocks; and (b) relationship between the predominant periods of the mainshocks ($T_{g,M}$) and their corresponding aftershocks ($T_{g,MA}$).

four earthquake scenarios occurred in California are shown in Fig. 11. Sample coefficient of correlation is also shown in the same figure. It can clearly be seen that the strong motion duration of the aftershocks is not correlated with their counterpart strong motion duration of the mainshocks. Furthermore, it was observed that strong-motion duration in the mainshocks was longer than that of the aftershocks ground motions in all examined sequences of the Imperial Valley and Mammoth Lakes, while it was longer about 91% and 58% for the far-field and near-fault examined sequences of the Northridge earthquakes.

4. Influence of the Aftershock Frequency Content in Structural Response

Most of the previous studies focused on the dynamic response of structures under mainshock-aftershock seismic sequences employed artificial seismic sequences instead of as-recorded seismic sequences. A common assumption in several previous studies was that the ground motion features (the amplitude, frequency content, and strong motion duration) of the mainshock acceleration time history are the same as that of the aftershock acceleration time history [Amadio *et al.*, 2003; Fragiaco *et al.*, 2004; Lee and Foutch, 2004; Hatzigeorgiou and Beskos, 2009; Erochko *et al.*, 2011]. Another assumption for generating artificial seismic sequences is that mainshock acceleration time histories randomly

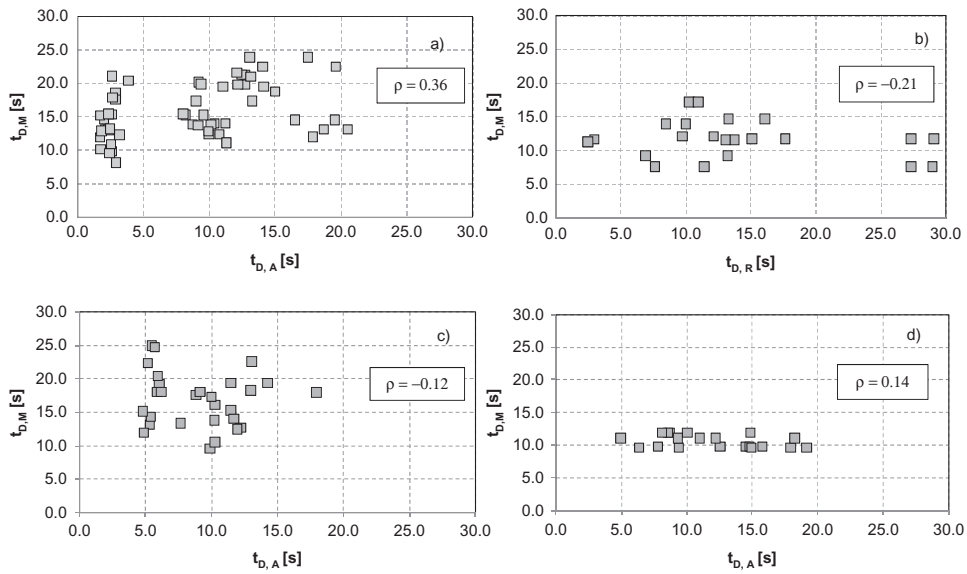


FIGURE 11 Strong-motion duration relationship of mainshock and for aftershocks: (a) 1994 Northridge earthquakes (far-field ground motions); (b) 1994 Northridge earthquakes (near-fault ground motions); (c) 1979 Imperial Valley earthquakes; and (d) 1980 Mammoth Lakes earthquakes.

selected from a ground motion catalog are employed as corresponding aftershocks, scaled or not scaled (e.g., [Luco *et al.*, 2004](#); [Li and Ellingwood, 2007](#); [Hatzigeorgiou, 2010](#); [Hatzigeorgiou and Liolios, 2010](#)). The latter approach is aimed at representing the stochastic relationships observed in as-recorded mainshock and corresponding aftershock acceleration time histories.

From quantitatively examining the seismic sequences included in this study, it is evident that the ground motion features between the mainshock and the following aftershocks are different for all seismic scenarios. Therefore, it can be concluded that the simulation approach of repeating the mainshock with the same amplitude, or reduced amplitude, to simulate an aftershock is not appropriate, even for mainshocks having the same fault mechanism. Instead, the randomized approach seems rational for generating artificial seismic sequences including the differences in ground motion features. However, it should be noted that for most earthquakes, the frequency content of the aftershocks is consistently higher than the frequency content of the corresponding mainshock (i.e., aftershocks have shorter predominant period of the ground motion than the mainshocks), which is the case of the seismic sequences recorded during the 1979 Imperial Valley earthquake and the 1994 Northridge earthquake. This issue could lead to wrong conclusions about the seismic response of structures.

To illustrate the importance of the ground motion characteristics of mainshock-aftershock sequences in the buildings response, let's consider the response of a four-story, three-bay, steel frame building when subjected to real and artificial sequences. The study-case frame was designed according to the 1994 Uniform Building Code for a structure located in zone 4 and it has a fundamental period of vibration equal to 1.23 s and yield strength coefficient equal to 0.32. Details of the frame model are given in [Ruiz-García and Negrete-Manriquez \[2011\]](#). The computer software RUAUMOKO [[Carr, 2004](#)] was employed for computing the dynamic response of the study-case frame model.

The first example considers a real seismic sequence recorded at Station 958 (El Centro Array 8), component 140, during the 1979 Imperial Valley earthquakes and two artificial sequences generated from the repeated and the randomized approach (employing the mainshock acceleration time-history, component 090, recorded at Convict Creek station during the 1980 Mammoth Lakes earthquake). The seismic sequences considered in this example are shown in Fig. 12 indicating the computed predominant period of the ground motion. It should be noted that while the real sequence has a ratio of the peak ground acceleration of the aftershock to the peak ground acceleration of the mainshock, $(PGA)_A/(PGA)_M$, equal to 0.20, the randomized sequence has a ratio equal to 0.69.

Figure 13 shows the response at the roof level corresponding to each seismic sequence. From this figure, it can be seen that the response triggered by the artificial sequences is very different from that due to the as-recorded seismic sequence. It should be noted that the artificial sequences overestimate peak displacements triggered by the real aftershock. An interesting observation is that permanent displacements at the end of the aftershocks are almost the same as those at the end of the mainshock, in spite of the larger intensity of the artificial aftershocks (i.e., artificial sequences have $(PGA)_A/(PGA)_M$ ratio greater than that of the real sequence).

In order to show the importance of the frequency content of the aftershock in the dynamic response of the structures, let's consider now the response of the same four-story frame building when subjected to a real seismic sequence recorded at Station CHP,

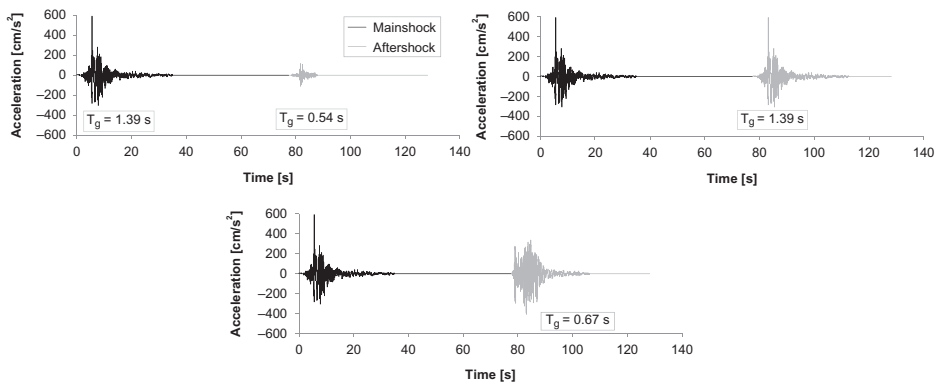


FIGURE 12 Comparison of seismic sequences: (a) real sequence recorded at El Centro Array 8 station (comp. 140) from the 1979 Imperial Valley earthquakes; (b) repeated (back-to-back) case; and (c) randomized case.

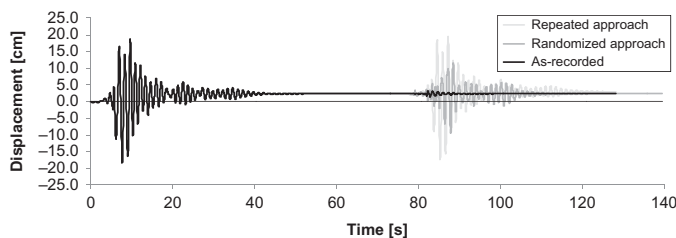


FIGURE 13 Displacement time-history response of a four-story frame model from a real sequence recorded at El Centro Array 8 (comp. 140) station during the 1979 Imperial Valley earthquakes and from two artificial seismic sequences.

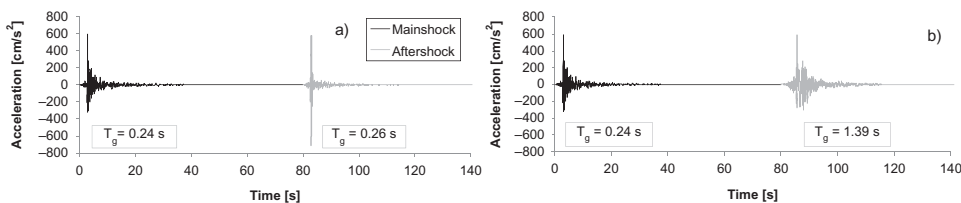


FIGURE 14 Comparison of seismic sequences: (a) real sequence recorded at CHP (comp. 090) station during the 1983 Coalinga earthquakes; and (b) randomized case.

component 090, during the 1983 Coalinga earthquakes and the artificial sequence generated from the randomized approach when employing the mainshock acceleration time-history recorded at El Centro Array 8, component 140, during the 1979 Imperial Valley mainshock earthquake as the following aftershock. Similarly, the seismic sequences are shown in Fig. 14 noting the computed predominant period of each ground motion. It should be noted that while the real sequence has a $(PGA)_A/(PGA)_M$ ratio equal to 1.21, the randomized sequence has a ratio equal to 0.99. That is, both sequences have strong aftershocks, but with very different predominant periods.

The displacement time-history response at the roof level corresponding to each seismic sequence is shown in Fig. 15. From this figure, it can be observed that the frame did not experience inelastic behavior (i.e., the frame does not exhibit permanent displacements at the end of the excitation) neither from the real mainshock nor from the aftershock in spite of the relatively large PGA of the excitation. However, it can be observed that the artificial sequence not only triggers a different response, but also peak and permanent roof displacements are increased as a consequence of the artificial aftershock. In order to explain this differences in response, it should be noted that the artificial aftershock has longer predominant period of the ground motion, which is close to the first-mode period of vibration of the frame ($T_1/T_g = 0.88$), than the real aftershock. Therefore, it is evident the influence of the aftershock's frequency content in the post-mainshock response of the frame model. In particular, the permanent displacement accumulation due to aftershocks argued in Hatzigeorgiou and Liolios [2010] does not necessarily occur, even under strong aftershocks, but it should depend in the relationship between the predominant period of the aftershock and the building's period of vibration at the end of the mainshock.

The difference between the building's response under the real near-fault sequences and the artificial sequences is illustrated next. For this purpose, three acceleration time-histories

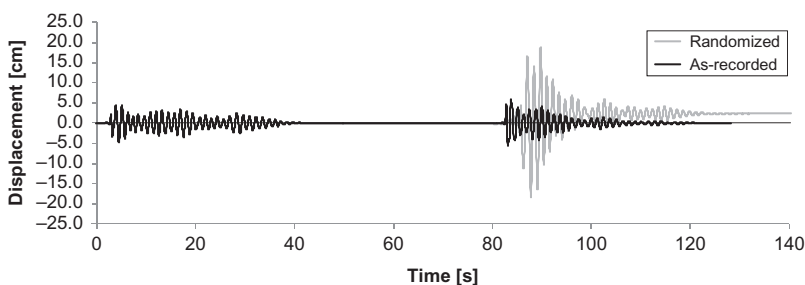


FIGURE 15 Displacement time-history response of a four-story frame model from a real sequence recorded at CHP (comp. 090) station during the 1983 Coalinga earthquakes and an artificial seismic sequence.

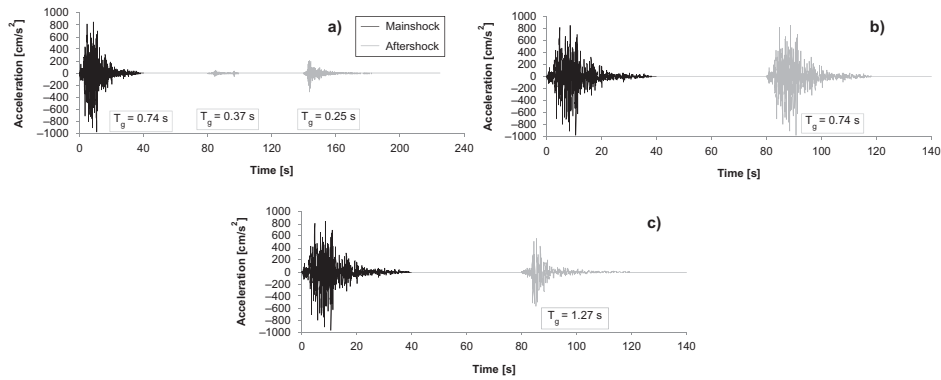


FIGURE 16 Comparison of seismic sequences: (a) real sequence recorded at Tarzana (comp. 360) station from the 1994 Northridge earthquakes; (b) repeated approach; and (c) randomized approach.

recorded at Tarzana Station (comp. 360) during the 1994 Northridge earthquakes are employed as shown in Fig. 16a. It should be noted that although the largest aftershock has a significant PGA (303 cm/s^2), the $(\text{PGA})_A/(\text{PGA})_M$ ratio is equal to 0.31 since the mainshock has a PGA of 971 cm/s^2 . The corresponding artificial sequences are shown in Figs. 16b–c. For generating the randomized case, the well-known acceleration time-history recorded at Newhall Fire Station (comp. 90) is added as artificial aftershock, that lead to a $(\text{PGA})_A/(\text{PGA})_M$ ratio is equal to 0.59. Note that the artificial aftershock has a predominant period close to the frame's fundamental period.

Figure 17 shows the displacement time-history response at the roof level corresponding to each seismic sequence. It can be seen that the frame experiences inelastic behavior due to the real mainshock triggering a small permanent displacement. It can also be observed that neither the peak nor the permanent displacements increase as a consequence of the aftershocks, which mean that the mainshock dominates the response. However, the response under artificial sequences is very different and they lead to larger peak displacements than the as-recorded sequence. It is interesting to note that the randomized approach leads to larger peak displacement demand than the repeated approach since the artificial aftershock might have similar predominant period of the ground motion than the period of the frame after the mainshock, which is particularly true since the frame experienced nonlinear behavior, even though the repeated approach assumes larger PGA than the randomized approach.

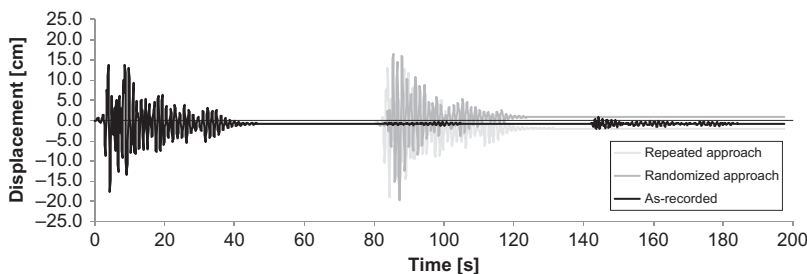


FIGURE 17 Displacement time-history response of a four-story frame model under real seismic sequence recorded at Tarzana (comp.360) station during the 1994 Northridge earthquakes and two artificial sequences.

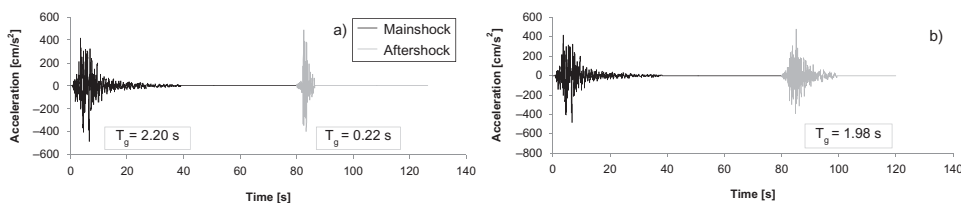


FIGURE 18 Comparison of seismic sequences: (a) real sequence recorded at Sylmar Converter station (comp. 288) from the 1994 Northridge earthquake; and (b) randomized approach.

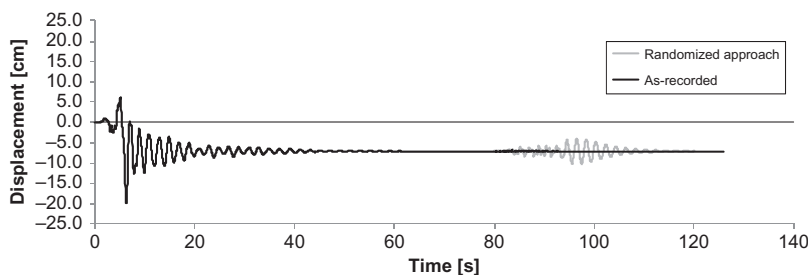


FIGURE 19 First-story displacement time-history response of an eight-story frame model under seismic sequences generated from the Sylmar Converter Station (comp.288).

Some of the near-fault mainshock ground motions have long predominant periods that might not trigger nonlinear behavior in the four-story frame model. Thus, a further look at the influence of the aftershock's frequency content is examined through the response of an 8-story frame model having a first-mode period of vibration equal to 1.95 s and yield strength coefficient equal to 0.25. The frame model is subjected to the sequence recorded at Sylmar Converter Station (comp. 288) and to an artificial sequence assembled with the mainshock acceleration time-history recorded at LA Baldwin Hills Station as an aftershock (comp. 90). To isolate the effect of the frequency content, the amplitude of both real and artificial aftershock ground motions were scaled up to $(PGA)_A/(PGA)_M$ ratio equal to one as shown in Fig. 18. The first-story displacement time-history under both sequences is shown in Fig. 19. It can be seen that even though the mainshock ground motion trigger permanent displacement at the first-story, the following aftershocks do not increase it. However, the transient response due to the artificial aftershock is larger than that of the real aftershock since the former has close predominant period than the frame's period of vibration.

Even though this study provides useful information about the response of structures under real seismic sequences, it should be recognized that previous observations were based in limited study-cases and they should be confirmed from additional analytical studies that incorporate frame models with different building's characteristics (e.g., different fundamental periods of vibration).

5. Conclusions

The dynamic response of man-made structures subjected to mainshock-aftershock seismic sequences has gained the attention of several investigations recently. For this task, input earthquake ground motions are of paramount importance. Thus, this article presented the

results of examining relevant ground motion characteristics of a relatively large suite of mainshock and corresponding aftershocks ground motion sequences recorded in accelerographic stations around the world. For this purpose, an ensemble of 184 real seismic sequences was identified from the Pacific Earthquake Engineering Research Center strong motion database and the Mexican Database of Strong Motions. In addition, the dynamic response of a low-height steel frame building under as-recorded and artificial seismic sequences was examined carefully to highlight the influence of the frequency content in the response. Although additional analytical studies employing different structural systems (e.g., reinforced concrete frames or masonry structures) and dynamic characteristics are still needed, this study provided useful insight about the response of framed structures under real seismic sequences. The following conclusions are drawn from this investigation.

In the first part of this study, it was found that the predominant period, which is a measure of the frequency content of the ground motion, of the examined mainshock ground motions is consistently longer than those of their corresponding largest aftershocks, which is particularly true for the 1979 Imperial Valley and 1994 Northridge earthquakes. This conclusion is consistent with seismological findings which suggest that aftershocks are triggered by rupturing small asperity areas in a fault plane after the mainshock event and, as a consequence, aftershock ground motions are richer in higher frequencies than mainshock ground motions.

Furthermore, this study showed that predominant periods of mainshocks and aftershocks are mildly-to-weakly correlated (from a statistical point of view). In addition, strong-motion duration was also found weakly correlated between mainshock and aftershock ground motions. Thus, there is no evidence that support generating artificial seismic sequences using the mainshock as a seed for reproducing the aftershock, even with reduced amplitude since the frequency content and strong-motion duration are different.

In the second part of this study, it was demonstrated that the dynamic response, measured by the lateral displacement demand, of a four-story and a eight-story steel frames subjected to artificial sequences derived from real mainshock ground motion, either from the repeated and the randomized approach, lead to a very different response than that when using real sequences. In particular, it was shown that the frequency content of the aftershock has strong influence in the dynamic post-mainshock response of the analyzed frames, measured by the peak and permanent displacement demand.

Based on the main findings of this investigation, it appears vital to use real seismic data for assessing the performance of existing structures under seismic sequences to take into account source mechanisms. In the absence of real seismic data, the randomized approach for generating artificial sequences should adequately reproduce the ground motion feature relationships between the mainshock and aftershock for conducting dynamic analysis of structures. That is, the set of artificial aftershock ground motions not only should have smaller amplitude than the real mainshock ground motion, but also most of them should have shorter predominant period.

Acknowledgments

The author would like to express his recognition to Mr. Juan C. Negrete-Manriquez and Mr. Apolo Maldonado for compiling the mainshock-aftershock catalogs considered in this study. In addition, financial support from *Universidad Michoacana de San Nicolás de Hidalgo* and the *Consejo Nacional de Ciencia y Tecnología* (CONACYT) in Mexico for developing the research reported in this article is greatly appreciated. Finally, the author would like to thank the comments and suggestions of two anonymous reviewers that helped to improve the final version of the article.